# Quasiclassical trajectory theoretical study on the chemical stereodynamics of the $O(^1D) + H_2 \rightarrow OH + H$ reaction and its isotopic variants (HD, $D_2$)

Yao Cui-Xia(姚翠霞) and Zhao Guang-Jiu(赵广久)†

*State Key Laboratory of Molecular Reaction Dynamics and Center for Theoretical and Computational Chemistry, Dalian Institute of Chemical Physics, Chinese Academy of Sciences, Dalian* 116023, *China*

(Received 2 December 2012; revised manuscript received 12 January 2013)

The quasiclassical trajectory (QCT) method is used to study stereodynamic information about the reaction $O(^1D) + H_2 \rightarrow OH + H$ on the DK (Dobbyn and Knowles) ($1^1A'$) *ab initio* potential energy surface (PES). A wide scale of collision energy ($E_c$) from 0.05 eV to 0.5 eV is considered in the dynamic calculations. To reveal the rovibrational excitation effect, calculations at a collision energy of 0.52 eV are carried out for the $v = 0 \sim 5$, $j = 0$ and $v = 0$, $j = 0 \sim 15$ initial states. The two popularly used polarization-dependent differential cross sections (PDDCSs), $d\sigma_{00}/d\omega_t$ (0, 0) and $d\sigma_{20}/d\omega_t(2, 0)$, and two angular distributions, $P(\theta_r)$ and $P(\varphi_r)$ are calculated to obtain an insight into the alignment and the orientation of the product molecules. From the calculations, we can obtain that the alignment of the OH product is weaker at high collision energy and becomes stronger with the increase of initial vibrational level, and it is almost insensitive to the initially rotational excitation. Influences of the mass values of isotopes (HD, $D_2$) on the stereodynamics are also shown and discussed. Comparisons between available theoretical results and experimental results are made and discussed.

**Keywords:** chemical stereodynamics, quasiclassical trajectory, vibrational and rotational excitation, product alignment and orientation

**PACS:** 34.70.+e, 32.10.Bi, 82.30.Fi, 34.50.Lf **DOI:** 10.1088/1674-1056/22/8/083403

## 1. Introduction

The electronically excited O ($^1D$) atom is an important chemical reagent in both atmospheric and combustion chemistry. The $O(^1D) + H_2/HD/D_2$ reactions are the simplest chemical reactions involving the electronically excited $O(^1D)$ atom.[1,2] Besides, the $O(^1D) + H_2$ reaction is a typical insertion reaction in chemical kinetics and reaction dynamics.[3] Different from direct abstraction reactions, the dynamic insertion reaction supported by a potential well can be much more complex because of the existence of numerous metastable resonances. The title reactions have been the target of experimental and theoretical researchers due to their fundamental significance.[4–7]

Experimentally, Liu *et al.*[8] have made a breakthrough so that the quantum state resolution for the differential cross section (DCS) can be obtained, which is comparable to detailed quantum mechanical (QM) results. All experiments confirmed that the title reactions are dominated by the insertion pathway on the ground state potential energy surface (PES).[9,10] To understand the reaction dynamics, theoretical efforts to determine the PES and dynamic studies using both QCT and QM methods have been made.[11–20] Although five potential energy surfaces (PESs) are accessible for the $O(^1D) + H_2$ reaction,[21] the main contribution stems from the lowest PES ($1^1A'$), favoring the formation of water. The DK PES, developed by Dobbyn and Knowle,[22] is one of the most popular *ab initio* PESs for $1^1A'$ state. The DK PES presents a potential well, and favors the insertion of O into the $H_2$ bond, rather than direct collisions of O with either end of the $H_2$ molecule.

The QCT method can be used to determine the polarization parameters as shown in Refs. [23]–[28]. Many studies about the title reactions have been conducted, however, the stereodynamics of these reactions on the DK PES still attract much attention. In the present work, the investigation of the product rotational polarization is carried out on the DK PES by considering influences of the collision energy, the initial vibrational states ($v = 0 \sim 5$, $j = 0$), and the initial rotational states ($v = 0$, $j = 0 \sim 15$). The HD and $D_2$ isotopic variants have also been studied by the QCT method on the same potential energy surface.

## 2. Theoretical methods

We use the centre-of-mass (CM) coordinate to describe the $\boldsymbol{k}$, $k'$, $\boldsymbol{j}'$ correlations as can be seen in Fig. 1.[29–34] The reagent ($H_2/HD/D_2$) relative velocity vector $\boldsymbol{k}$ is parallel to the $z$ axis, the $x$–$z$ plane is considered as a scattering plane, which contains the initial and final relative vectors $\boldsymbol{k}$, $\boldsymbol{k}'$. Angle $\theta_t$ is the known scattering angle between the $\boldsymbol{k}$ and $\boldsymbol{k}'$, $\theta_r$ the polar, and $\varphi_r$ the azimuthal angle of product rotational momentum $\boldsymbol{j}'$.

†Corresponding author. E-mail: gjzhao@dicp.ac.cn

© 2013 Chinese Physical Society and IOP Publishing Ltd 

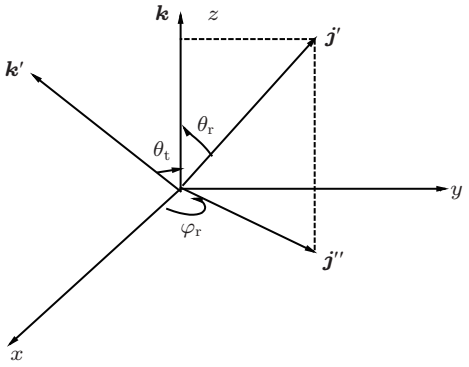



**Fig. 1.** Centre-of-mass coordinate system used to describe the $\boldsymbol{k}$, $\boldsymbol{k}'$, $\boldsymbol{j}'$ direcations.

The fully correlated angular distribution can be written as follows:[35–37]

$$P(\cos\theta_{\rm t},\cos\theta_{\rm r},\varphi_{\rm r}) = \frac{1}{4\pi}\sum_{k=0}^{\infty}\sum_{q=-k}^{k}(2k+1)\frac{2\pi}{\sigma}\frac{{\rm d}\sigma_{kq}}{{\rm d}\omega_{\rm t}}C_{kq}(\theta_{\rm r},\varphi_{\rm r}). \quad (1)$$

Here is a series of generalized polarization-dependent differential cross sections (PDDCSs).

The $P(\theta_{\rm r})$ describes the $\boldsymbol{k}$–$\boldsymbol{j}'$ vector correlation and can be expanded in a series of Legendre polynomials as follows:

$$P(\theta_{\rm r})=\frac{1}{2}\sum_{k}[k]\,\langle {\rm P}_k(\cos\theta_{\rm r})\rangle P_k(\theta_{\rm r}), \quad (2)$$

and

$$\langle {\rm P}_k(\cos\theta_{\rm r})\rangle=\int_0^{\pi}{\rm P}(\theta_{\rm r}){\rm P}_k(\cos\theta_{\rm r})\sin\theta_{\rm r}{\rm d}\theta_{\rm r}=a_0^{(k)}. \quad (3)$$

The integer $k$ is 18, and this ensures the convergent result of $P(\theta_{\rm r})$.

The dihedral angle distribution function $P(\varphi_{\rm r})$ describes the $\boldsymbol{k}$–$\boldsymbol{k}'$–$\boldsymbol{j}'$ vector correlations, which can be expanded in a Fourier series as follows:

$$P(\varphi_{\rm r}) = \frac{1}{2\pi}\left(1+\sum_{\text{even},n\geqslant 2}a_n\cos n\varphi_{\rm r}+\sum_{\text{odd},n\geqslant 1}b_n\sin n\varphi_{\rm r}\right). \quad (4)$$

The integer $n$ is chosen to be 24 for a good convergence.

The QCT method used in our paper is the same as the one used in previous studies.[26–28,38–40] For each collision energy, $10^4$ trajectories are run on the DK PES. The intergration step size in the trajectories is chose to be 0.1 fs, which is sufficient for the total energy and angular momentum conservation. The initial distance from O to the center of $H_2$/HD/$D_2$ is chosen to be 10 Å (1 Å = 0.1 nm).

## 3. Results and discussion

The calculated PDDCS$_{00}$ and PDDCS$_{20}$ ($d\sigma_{00}/d\omega_t$, $d\sigma_{20}/d\omega_t$) from the O + $H_2$ ($v = 0$, $j = 0$) reaction, each of which is plotted as a function of both collision energy ($E_c$) and scattering angle $\theta_t$, are shown in Figs. 2 and 3. To the best of our knowledge, the PDDCS$_{00}$ correlates with the differential cross section ($\boldsymbol{k}$, $\boldsymbol{k}'$). As can be seen in the figure, the PDDCS$_{00}$ we obtained is sensitive to the collision energy. For low collision energy, i.e., when $E_c \leq 0.14$ eV, the distribution of product OH molecules is nearly forward–backward symmetric. The angular distribution shown for low collision energy indicates that the O + $H_2$ reaction is a typical reaction with a complex-forming mechanism. With the further increase of collision energy, the OH product molecules are obviously backward scattered, and such a backward scattering becomes more important when $E_c = 0.5$ eV. PDDCS$_{20}$ is representative of the expectation value of the second Legendre moment $\langle {\rm P}_2(\cos\theta_{\rm r})\rangle$. Compared with results in Fig. 2, the distribution of PDDCS$_{20}$ in Fig. 3 has a trend opposite to that of PDDCS$_{00}$. In addition, we can also conclude that product rotational momentum $\boldsymbol{j}'$ is preferentially polarized along the direction perpendicular to $\boldsymbol{k}$ when $\theta_t = 0°$ or $\theta_t = 180°$, because it has the most negative value of −0.35 at these two angles for all collision energies, which is close to −0.5. Furthermore, PDDCS$_{20}$ shown here is found to be nearly independent of collision energy.

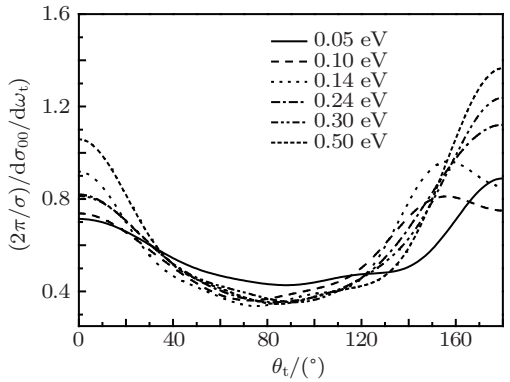



**Fig. 2.** Values of product polarization-dependent differential cross-section PDDCS$_{00}$ of the reaction O + $H_2$ ($v = 0$, $j = 0$)→OH + H for six different collision energies.

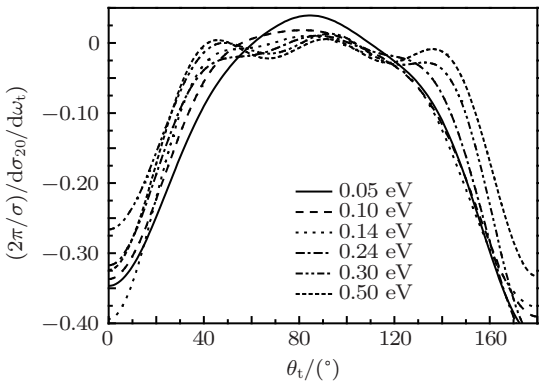



**Fig. 3.** Values of product polarization-dependent differential cross-section PDDCS$_{20}$ of the reaction O + $H_2$ ($v = 0$, $j = 0$)→OH + H for six different collision energies.

To obtain a better graphical representation of product polarization for the OH product from the $O(^1D)+H_2$ ($v=0$, $j=0$)$\rightarrow$OH + H reaction, we plot the distributions of $P(\theta_r)$ and $P(\varphi_r)$ for six different collision energies in Figs. 4 and 5, respectively. As illustrated in Fig. 4, the peak of $P(\theta_r)$ appears near $\theta_r = 90^\circ$ and is symmetric around $\theta_r = 90^\circ$ for all energies, which states that the OH product angular momentum $\boldsymbol{j}'$ is aligned along the direction perpendicular to the relative velocity $\boldsymbol{k}$. The peaks of the $P(\theta_r)$ distribution almost keep unchanged when collision energy changes from 0.05 eV to 0.14 eV. As collision energy increases further, $P(\theta_r)$ distribution becomes broader and lower, indicating the product molecule alignment becomes weaker at high collision energy. Figure 5 shows the $P(\varphi_r)$ distributions at six collision energies of 0.05, 0.1, 0.14, 0.24, 0.3, and 0.5 eV. It is clear that the distribution of $P(\varphi_r)$ is asymmetric with respect to the $\boldsymbol{k}$–$\boldsymbol{k}'$ scattering plane, and the main peaks appear at $\varphi_r = 90^\circ$ and $\varphi_r = 270^\circ$, indicating that the rotational angular momentum vectors of the OH product molecule are mainly aligned along the $y$ axis and the O + $H_2$ reaction is mainly governed by the 'in-plane' mechanism. Expect for $E_c = 0.5$ eV, the peak of $P(\varphi_r)$ appearing at $\varphi_r = 90^\circ$ is nearly the same as at $\varphi_r = 270^\circ$. This observation means that the orientation of the product OH has no obvious tendency along the positive $y$ axis, nor along the negative $y$ axis. For $E_c = 0.5$ eV, there is a relatively strong peak at $\varphi_r = 90^\circ$, which means that the $\boldsymbol{j}'$ of the product OH is not only aligned, but also oriented along the positive $y$ axis.

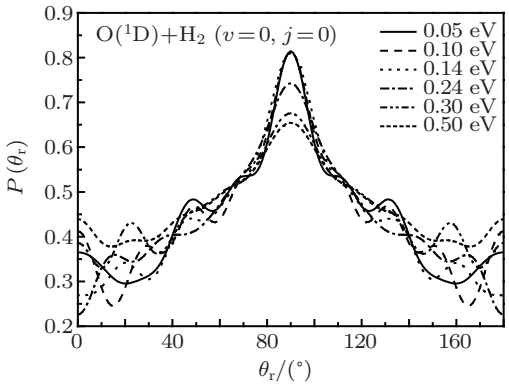



**Fig. 4.** Distributions of $P(\theta_r)$ for the O + $H_2$ ($v=0$, $j=0$)$\rightarrow$OH + H at six different collision energies, 0.05, 0.10, 0.14, 0.24, 0.3, and 0.5 eV.

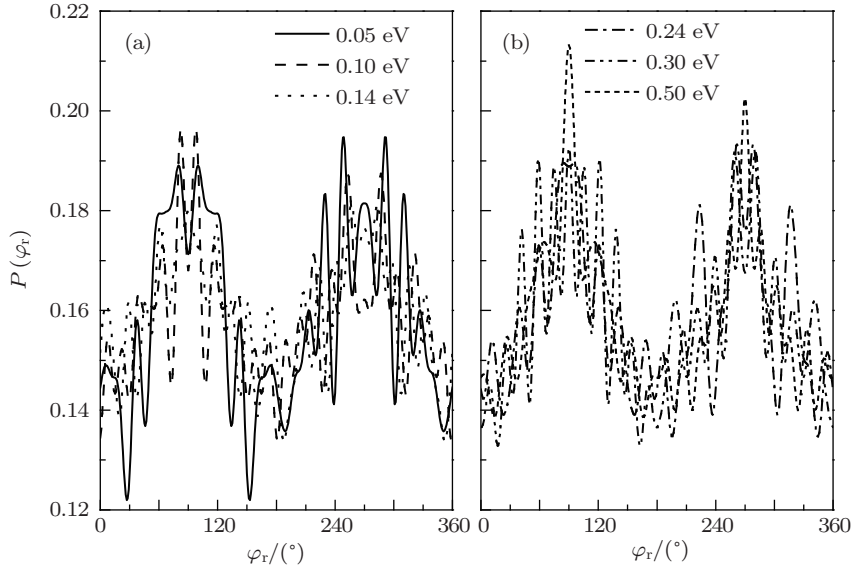



**Fig. 5.** Distributions of $P(\varphi_r)$ for the product molecule OH from the reaction $O(^1D)+H_2$ ($v=0$, $j=0$)$\rightarrow$OH + H at six different collision energies, (a) 0.05, 0.10, and 0.14 eV; (b) 0.24, 0.3, and 0.5 eV.

Figures 6(a) and 6(b) show the distributions of $P(\theta_r)$ for the $O(^1D)+H_2$ ($v=0\sim5$, $j=0$; $v=0$, $j=0\sim15$) reaction at a collision energy of 0.52 eV. As can be seen in Fig. 6, all the peaks of $P(\theta_r)$ distributions exist around $\theta_r = 90^\circ$, which indicates that the product OH angular momenta align in the direction perpendicular to $\boldsymbol{k}$ for all the considered rovibrational levels. In Fig. 6(a), with the increase of vibration–excitation level, we can see a contraction in each of $P(\theta_r)$ distribution, and the peak of $P(\theta_r)$ at $\theta_r = 90^\circ$ shifts upward gradually. We can conclude that the initial vibration excitation is in favor of the product molecule alignment, and the vibration quantum number $v$ plays an important role in dynamical stereochemistry of the O ($^1$D) + $H_2$ $\rightarrow$ OH + H reaction. By contrast, Fig. 6(b) shows that the influence of the initial rotational excitation on $P(\theta_r)$ distribution is weaker than that of the vibration quantum number $v$. The dependence of the rotational quantum number $j$ on the $P(\theta_r)$ distribution is not obvious.

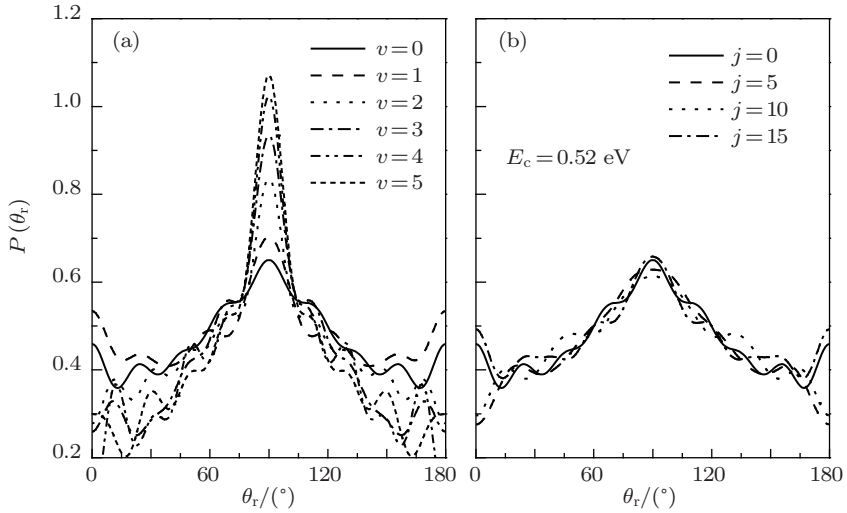



**Fig. 6.** Distributions of $P(\theta_r)$ as a function of the polar angle $\theta_r$ for different initial rovibrational states at $E_c = 0.52$ eV: (a) for the reactions $O + H_2$ ($v = 0 \sim 5$, $j = 0$); and (b) for the reactions $O + H_2$ ($v = 0$, $j = 0 \sim 15$).

For the O + HD→OH(D) + D(H) reaction, many dynamical features are the same except for the branching ratio of the integral cross section for both exit channels.[41–44] Table 1 presents the branching ratio $\Gamma_{OD/OH}$ for the reaction O + HD ($v = 0$, $j = 0$) on the DK PES in a wide collision energy range ($\Gamma_{OD/OH} = \sigma_{(OD+H)}/\sigma_{(OH+D)}$). Here, $\sigma_{(OD+H)}$ means the integral cross section (ICS) for the reaction O + HD→OD + H and $\sigma_{(OH+D)}$ represents ICS for the O + HD→OH + D reaction. We also present experimental data and available theoretical results obtained by using other PESs. As can be seen, the branching ratio of the integral cross section $\Gamma_{OD/OH}$ calculated on the DK PES is closer to the experimental results than that on the BR PES for $E_c = 0.09$ eV.[5,41,42] This comparison confirms the accuracy of the DK PES and the validity of this QCT method. Our findings also reveal a preference of the OD + H product channel over the OH + D product channel, and the branching ratio $\Gamma_{OD/OH}$ shows an increasing-then-decreasing trend over the whole collision energy range we considered. On the basis of this observation, we can see that this branching ratio has apparent connection with the collision energy and is generally dependent on the used PES.

**Table 1.** Isotopic ratios of integral cross section for the reaction $O(^1D) + HD \rightarrow OH(D) + D(H)$ from different PESs and corresponding experimental data ($\Gamma_{OD/OH} = \sigma_{(OD+H)}/\sigma_{(OH+D)}$).

| $E_{col}$/eV | $\Gamma_{OD/OH}$ | PES | Refs. |
|---|---|---|---|
| 0.05 | 1.681 | DK | this work |
| 0.07 | 1.689 | DK | this work |
| 0.09 | 1.921 | DK | this work |
| | 1.17±0.1 | exp. | [5], [42] |
| | 2.15±0.09 | BR | [41] |
| 0.1 | 1.908 | DK | this work |
| | 1.5±0.2 | exp. | [2] |
| 0.2 | 1.864 | DK | this work |
| 0.5 | 1.635 | DK | this work |

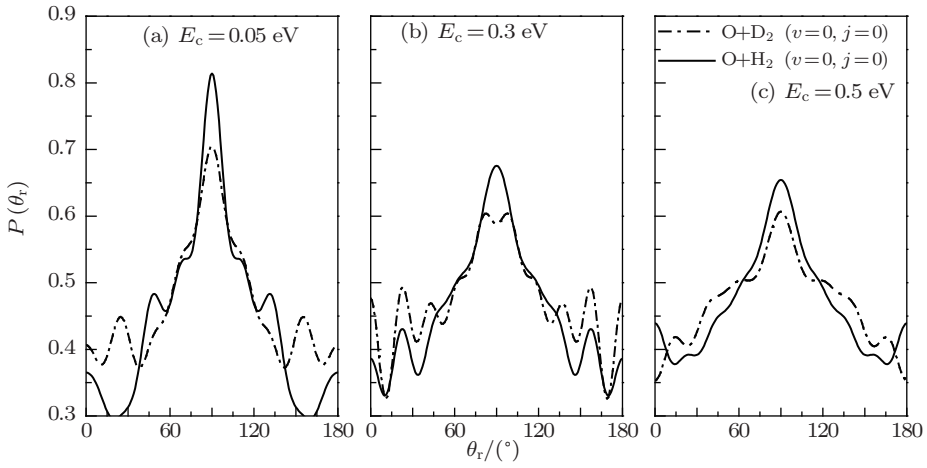



**Fig. 7.** Distributions of $P(\theta_r)$ for the product molecule from the reactions $O + H_2/D_2$ ($v = 0$, $j = 0$)→OH/OD + H/D at (a) $E_c = 0.05$ eV; (b) $E_c = 0.3$ eV; and (c) $E_c = 0.5$ eV.

Figure 7 presents the distributions of $P(\theta_r)$ for the reactions $O + H_2/D_2$ ($v = 0$, $j = 0$)$\rightarrow$OH/OD + H/D at three different collision energies of 0.05, 0.3, and 0.5 eV. Similarities and dissimilarities can be observed by comparing both reactions. As shown in Figs. 7(a)–7(c), all the peaks of the $P(\theta_r)$ are symmetric around $\theta_r = 90^\circ$, which fit well to the results in Figs. 4 and 6. In contrast to the $O + H_2$ reaction, the peaks of $P(\theta_r)$ become different after $H_2$ has been substituted by $D_2$. According to previous studies,[45–47] the discrepancy between the $P(\theta_r)$ distributions stems from the difference in mass factor ($\cos^2\beta = m_A m_c/(m_A + m_B)(m_B + m_c)$). The values of mass factor for $O + H_2$ and $O + D_2$ are 0.472 and 0.447, respectively. All the peaks of the $P(\theta_r)$ shift downward after $H_2$ has been substituted by $D_2$. It is clear that a larger mass factor will lead to stronger product molecule alignment, which is consistent with the results given by Zhao *et al*.[46]

## 4. Conclusions

We perform QCT calculations on the DK potential energy surface for the title reactions. Two commonly used PDDCSs ($PDDCS_{00}$ and $PDDCS_{20}$) and two angle distributions $P(\theta_r)$ and $P(\varphi_r)$ are plotted to investigate the stereodynamics of the $O(^1D) + H_2$ reaction together with its isotopic effect. For the $O + H_2$ ($v = 0$, $j = 0$) reaction, the angular distribution of product OH molecules is nearly forward–backward symmetric at low collision energies, when the collision energy increases, a backward scattering bias appears. The OH product alignment is weaker at high collision energy, becomes stronger with the increase of initial vibrational level, but it is almost insensitive to the initially rotational excitation. The trend of the distributions $P(\theta_r)$ for $O(^1D) + D_2$ is similar to for the reaction $O(^1D) + H_2$, but the peak of $P(\theta_r)$ around $\theta_r = 90^\circ$ for the $O + D_2$ reaction is lower than that for the $O + H_2$ reaction.

## References


[1] Anderson J G 1987 *Ann. Rev. Phys. Chem.* **38** 489
[2] Alexander A J, Blunt D A, Brouard M, Simons J P, Aoiz F J, Banares L, Fujimura Y and Tsubouchi M 1997 *Faraday Discuss.* **108** 375
[3] Ho T S, Hollebeek T, Rabitz H, Harding L B and Schatz G C 1996 *J. Chem. Phys.* **105** 10472
[4] Davidson J A, Sadowski C M, Schiff H I, Streit G E, Howard C J, Jennings D A and Schmeltekopf A. L 1976 *J. Chem. Phys.* **64** 57
[5] Hsu Y T, Wang J H and Liu K 1997 *J. Chem. Phys.* **107** 2351
[6] Brownbill S J and Softley T P 2005 *Mol. Phys.* **103** 2347
[7] Bell M T and Softley T P 2009 *Mol. Phys.* **107** 99
[8] Liu X H, Lin J J, Harich S A, Schatz G C and Yang X. M 2000 *Science* **289** 1536
[9] Hermine P, Hsu Y T and Liu K 2000 *Phys. Chem. Chem. Phys.* **2** 581
[10] Liu X H, Lin J J, Harich S A and Yang X Y 2001 *Phys. Rev. Lett.* **86** 408
[11] Chu T S and Han K L 2005 *J. Phys. Chem. A* **109** 2050
[12] Zhang Y, Xie T X and Han K L 2003 *J. Phys. Chem. A* **107** 10893
[13] Chu T S and Han K L 2008 *Phys. Chem. Chem. Phys.* **10** 2431
[14] Hu J, Han K L and He G Z 2005 *Phys. Rev. Lett.* **95** 123001
[15] Zhao G, Han K, Lei Y and Dou Y 2007 *J. Chem. Phys.* **127** 094307
[16] Chu T S, Zhang X and Han K L 2005 *J. Chem. Phys.* **122** 214301
[17] Wang W L, Rosa C and Brandao J 2006 *Chem. Phys. Lett.* **418** 250
[18] Zhu D H, Zhang B, Shen Y F and Dai K 2011 *Chin. Phys. Lett.* **28** 094301
[19] Chu T S, Zhang Y and Han K L 2006 *Int. Rev. Phys. Chem.* **25** 201
[20] Li Y J, Sun W G, Zeng Y Y, Wang X L, Li H D, Feng H and Fan Q C 2011 *Acta Phys. Sin.* **60** 043401 (in Chinese)
[21] Durand G and Chapuisat X 1985 *Chem. Phys.* **96** 381
[22] Dobbyn A J and Knowles P J 1997 *Mol. Phys.* **91** 1107
[23] Han K L, He G Z and Lou N Q 1991 *Chem. Phys. Lett.* **178** 528
[24] Han K L, He G Z and Lou N Q 1996 *J. Chem. Phys.* **105** 8699
[25] Wang M L, Han K L and He G Z 1998 *J. Phys. Chem. A* **102** 10204
[26] Zong F J and Xu Z H 2011 *Chin. Phys. B* **20** 063104
[27] Xu Y, Zhao J, Yue D G, Liu H, Zheng X Y and Meng Q T 2009 *Chin. Phys. B* **18** 5308
[28] Xu Z H, Zong F J, Han B R, Dong S H, Liu J Q and Ji F 2012 *Chin. Phys. B* **21** 093103
[29] Han K L, He G Z and Lou N Q 1993 *Chin. Chem. Lett.* **203** 509
[30] Han K L, He G Z and Lou N Q 1992 *Chin. J. Chem. Phys.* **96** 7865
[31] Sun G H, Yang X D, Zhu J and Wang C X 2002 *Chin. Phys.* **11** 910
[32] Xie T X, Zhang Y, Zhao M Y and Han K L 2003 *Phys. Chem. Chem. Phys.* **5** 2034
[33] Cheng J, Yue X F and Feng H R 2012 *Chin. Phys. Lett.* **29** 043101
[34] Xu W W and Zhao G J 2012 *Cent. Eur. J. Phys.* **10** 253
[35] Zhao G, Liu Y, Han K and Dou Y 2008 *Chem. Phys. Lett.* **453** 29
[36] Shaferray N E, Orrewing A J and Zare R N 1995 *J. Phys. Chem.* **99** 7591
[37] Kobayashi H, Takayanagi T and Tsunashima S 1997 *Chem. Phys. Lett.* **277** 20
[38] Han K L and He G Z 2007 *J. Photochem. Photobiol. C* **8** 55
[39] Chen T Y, Zhao N J, Zhang W P and Wang X Q 2011 *Cent. Eur. J. Phys.* **9** 1221
[40] Chen M D, Han K L and Lou N Q 2002 *Chem. Phys. Lett.* **357** 483
[41] Rio C M A and Brandao J 2007 *Chem. Phys. Lett.* **433** 268
[42] Lee S H and Liu K 1998 *Chem. Phys. Lett.* **290** 323
[43] Alexender A J, Aoiz F J, Brouard M and Simons J P 1996 *Chem. Phys. Lett.* **256** 561
[44] Fitzcharles M S and Schatz G C 1986 *J. Phys. Chem.* **90** 3634
[45] Zhao J, Xu Y and Meng Q T 2009 *J. Phys. B* **42** 165006
[46] Zhao J 2011 *Can. J. Chem.* **89** 650
[47] Wang M L, Han K L and He G Z 1998 *J. Chem. Phys.* **109** 5446